Clinical and Experimental Medicine (2026) 26:161
https://doi.org/10.1007/s10238-026-02058-x

RESEARCH

A proteomics approach to identify predictive blood biomarkers for pleural mesothelioma in prospective cohorts

Elton Jalis Herman[1] · Alessandra Allione[1] · Clara Viberti[1] · Marcello Manfredi[2] · Alessia Russo[1] · Khadija Sana-Hafeez[1] · Nina Kaiser[3] · Georg Johnen[3] · Thomas Brüning[3] · Dario Mirabelli[5] · Irma Dianzani[4,6] · Antonio Agudo[7,8] · Elisabete Weiderpass[9] · Vittorio Simeon[10] · Rudolf Kaaks[11] · Renée Turzanski-Fortner[11] · Rosario Tumino[12] · Lorenzo Milani[13] · José María Gálvez-Navas[14,15,16] · Matthias B. Schulze[17,18] · Catarina Schiborn[17,18,25] · Natalia Cabrera Castro[19,20] · Giovanna Masala[21] · Marcela Guevara[22,23,24] · Paolo Vineis[26] · Elisabetta Casalone[1] · Giuseppe Matullo[1,5,27]

Received: 6 November 2025 / Accepted: 12 January 2026

Abstract

Background Pleural mesothelioma (PM) is a rare, asbestos-linked cancer with a long asymptomatic latency, delaying diagnosis and limiting treatment options. Identifying blood-based biomarkers that signal disease before symptoms onset could improve surveillance of at-risk individuals.

Methods In our work, we conducted a prospective proteomic study of pre-diagnostic serum from 21 PM cases (<5 years before diagnosis) and 21 asbestos-exposed controls in the EPIC cohort using SWATH-MS, followed by ELISA validation. Findings were tested in an independent MoMar cohort of 32 pre-diagnostic plasma samples (<1 year before diagnosis) and 32 matched controls.

Results SWATH-MS identified 12 differentially expressed proteins (nominal $p<0.05$, fold change >1.3 or <0.75). Transferrin and complement C4A were elevated, while beta-2-microglobulin and dermcidin were reduced in pre-diagnostic cases. ELISA confirmed a borderline significant rise in beta-2-microglobulin within two years of diagnosis in EPIC. Calretinin and mesothelin were also detected in both cohorts, with the five-marker panel achieving an AUC of 0.91 ($p=0.001$) in MoMar but not reaching significance in EPIC (AUC = 0.88, $p=0.17$).

Conclusions Integrating novel proteomic biomarker candidates with established markers enhances early PM detection in high-risk populations. Larger, multi-cohort validation is warranted to refine this biomarker panel for clinical surveillance.

Keywords Pleural mesothelioma · Asbestos exposure · Multi-Cohort · Prospective study · Proteomics · Early biomarkers.

Abbreviations

AUC	Area under curve
B2M	Beta-2-Microglobulin
CO4A	Complement 4 A
DCD	Dermicidin
DDA	Data-dependent acquisition
DEPs	Differentially expressed proteins
DIA	Data-independent analysis
EPIC	European Prospective Investigation into Cancer and Nutrition cohort
EI	Exposure index
FC	Fold change
GLM	Generalized linear model
ICD	International Statistical Classification of Diseases, Injuries and Causes of Death
ISVF	Ion spray voltage floating
JEM	Job-exposure matrix
MoMar	Molecular markers for early detection of cancer

Elton Jalis Herman and Alessandra Allione contributed equally to this work and share first authorship.

Extended author information available on the last page of the article

Published online: 20 February 2026

PM Pleural Mesothelioma
SWATH MS Sequential Window Acquisition of all Theoretical Mass Spectra
TF Transferrin
TTD Time to diagnosis

Introduction

Pleural Mesothelioma (PM) is an aggressive, rare malignancy of the pleural cavity with a median survival of approximately 12 months [1, 2]. The primary etiological factor is exposure to asbestos fibers, particularly the amphibole subtypes crocidolite and anthophyllite, which predominate in lung tissue, correlate with asbestos fiber burden, and influence disease prognosis [3, 4]. Despite advances in genomic and molecular profiling over the past decade aimed at identifying therapeutic targets [5–7], and growing clinical interest in immunotherapy [8], patient outcomes remain poor.

Early diagnosis could extend the potential window for preventive interventions, yet no reliable screening methods exist for PM. The long latency period between asbestos exposure and disease onset, combined with nonspecific symptoms, renders detection in the pre-clinical phase exceptionally challenging [9, 10].

Proteomics offers a promising avenue for discovering biomarkers capable of detecting early-stage tumors and refining prognostic assessments over time. Cancer detection hinges on identifying deviations from normal physiology before clinical manifestation, requiring predictive markers in readily accessible biological samples that can be obtained through minimally invasive procedures [11, 12]. However, most proteomic studies in PM have analyzed samples collected at or after diagnosis, potentially capturing disease consequences rather than predictive signals, a limitation that introduces reverse causality. Whether these biomarkers can identify pleural lesions during the latent phase in asbestos-exposed individuals remains uncertain [13]. Proteomic profiling has the potential to reveal aberrant protein expression patterns at critical timepoints, enabling surveillance of at-risk populations and facilitating early PM diagnosis [14]. Proteins occupy a unique position at the interface of genotype and phenotype, integrating genetic and environmental influences including lifestyle and occupational exposures on clinical outcomes [15]. This is particularly relevant in heterogeneous malignancies like PM, where proteomics bridges the gap between genomic, transcriptomic, and phenotypic data. Although numerous blood-based biomarkers have been identified across various cancers, few have achieved clinical implementation due to insufficient specificity and reproducibility. The search for the ultimate panel of protein biomarkers continues, necessitating more sophisticated analytical approaches to the proteomic habitat. Investigating biofluid proteomes in a time sensitive manner is therefore critical for enhancing risk stratification in vulnerable populations and elucidating the molecular pathways underlying disease initiation [16, 17].

Materials and methods

EPIC study design and population (discovery and validation)

European Prospective Investigation into Cancer and Nutrition (EPIC) cohort is a multi-center cohort study, conducted in 23 centers across 10 European countries, aimed at investigating the etiological role of biological, lifestyle, and environmental factors in cancer and other chronic diseases. Overall, 521,468 healthy participants were enrolled in EPIC, and followed-up on an ongoing basis [18]. Within the EPIC cohort, 135 participants developed PM (EPIC-Meso) after a mean follow-up of 8.3 years (range 0.5–18.8 years). The disease was classified using ICD-10 diagnosis codes (ICD, International Statistical Classification of Diseases, Injuries and Causes of Death) as C38.4 (malignant neoplasm of pleura) in all participants. Cancer endpoint data (time of PM diagnosis) is based on the latest round of follow-up received from the EPIC centers and centralized at IARC between 2014 and 2016. For this specific study we selected those participants who were diagnosed with PM within 5 years after enrolment in the cohort (n = 21). Pre-diagnostic proteomic profiles of their single blood serum samples, taken at enrolment, were compared to those of matched healthy controls with no cancer diagnosis or other comorbidities present at the time of proteomic profiling. The controls were selected to match the cases by sex, age at enrolment (± 1.5 years), study center, and asbestos-exposure (see "Asbestos-exposure assessment" section). Blood collection, processing and storage were performed following a strict protocol [18, 19].

Molecular marker (MoMar) cohort (Replication)

For the replication of biomarkers discovered in EPIC pre-diagnostic individuals, we chose participants from the MoMar cohort study [20]. All 2.769 participants of the MoMar study were former asbestos workers with recognized occupational diseases (benign asbestos-related diseases like asbestosis, pleural plaques etc.) who, between 2008 and 2018, were invited to annual health examinations that included blood sampling and a questionnaire. Most of

the participants were men, only 0.7% were women. Recruitment of this high-risk group [21] took place at 26 centers across Germany and led to 12,548 examinations with corresponding serial plasma and full blood samples that were stored in a central biobank at -150 °C. A follow-up in 2019 resulted in 43 confirmed mesothelioma cases. For the current study, we compared the pre-diagnostic blood plasma samples of the 43 cases (of each case series the last available sample before diagnosis) to those of control participants drawn from the same cohort. The controls were carefully matched to the cases in terms of sex (all cases were male) and age at sampling. The cases were divided into the time intervals > 0 to 2 years and > 2 to 5 years before diagnosis (39 and 4 cases, respectively) as well as into 1-year intervals (Table 3).

It is important to note that both EPIC and MoMar are established as prospective cohorts with forward-looking enrollment and biobanking protocols, the laboratory proteomic and ELISA analyses were performed retrospectively on stored pre-diagnostic samples. However, the critical prospective feature of both cohort's collection of blood samples before any cancer diagnosis in participants who later developed PM eliminates reverse causality and provides the essential temporal relationship for identifying pre-diagnostic biomarkers.

Asbestos-exposure assessment in EPIC cohort

Occupational information was available from the baseline EPIC questionnaire. It included the occupation at enrolment and data on ever working up to the time of enrolment in 52 at-risk occupations. No information was available on duration of employment and time of first employment. A semi-quantitative job-exposure matrix (JEM) was developed by expert epidemiologists as previously described [22] assigning an "exposure probability" and an "exposure intensity" score to each of the 52 EPIC occupational categories. Both scores were expressed over a numerical scale with four levels: 0 "no exposure", 1 "low", 2 "intermediate", 3 "high" and multiplied to generate an Exposure Index (EI). For the present study, we used a categorical variable with 3 levels defined as "no exposure" (EI = 0), "low exposure" (EI = 1), and "high exposure" (EI = 2).

Sample Preparation for mass spectrometry

Serum samples from EPIC individuals were depleted of the high-abundance proteins (serum albumin (HSA), IgG, IgA, IgM, IgD, IgE, kappa and lambda light chains, alpha-1-acid glycoprotein, alpha-1-antitrypsin, alpha-2-macroglobulin, apolipoprotein A1, fibrinogen, haptoglobin, transferrin) using the Seppro IgY14 spin column kit (Sigma-Aldrich Inc., St. Louis, MO, USA) according to the manufacturer's procedure. The samples were then subjected to denaturation with TFE, to reduction with DTT 200 mM, to alkylation with IAM 200mM and to complete protein digestion with 1 µg of Trypsin (Sigma-Aldrich Inc., St. Louis, MO, USA). Next, peptides were desalted on the Discovery® DSC-18 solid phase extraction (SPE) 96-well plate (25 mg/well) (Sigma-Aldrich Inc., St. Louis, MO, USA). A labelled peptide was added to assure the reproducibility of the sample preparation and acquisition. Additional quality control samples were run to ensure the quality of the analysis.

Sequential window acquisition of all theoretical mass spectra (SWATH MS/MS) analysis of samples

Samples were analysed using a data-dependent acquisition (DDA) followed by data-independent analysis (DIA) through a micro-LC Eksigent Technologies (Eksigent, Dublin, USA) system interfaced with a 5600 + TripleTOF system (AB Sciex, Concord, Canada). Digested peptides were separated using Halo C18 column (0.5 × 100 mm, 2.7 µm; Eksigent Technologies Dublin, USA). The reverse phase LC solvents include solvent A (99.9% water + 0.1% formic acid) and solvent B (99.9% acetonitrile + 0.1% formic acid). A 30 min gradient was used at a flow rate of 15 µL/min with an increasing concentration of solvent B from 2% to 40%. For DDA acquisition, experiments were set to obtain a high-resolution TOF-MS scan over a mass range of 100–1500 m/z, followed by an MS/MS product ion scan from 200 to 1250 Da (accumulation time of 5.0 ms) with the abundance threshold set at 30 cps (35 candidate ions can be monitored during every cycle). The ion source parameters in electrospray positive mode were set as follows: curtain gas (N2) at 25 psig, nebulizer gas GAS1 at 25 psig, and GAS2 at 20 psig, ion spray voltage floating (ISVF) at 5000 V, source temperature at 450 °C and declustering potential at 25 V. Using the same conditions as described above, a SWATH acquisition using DIA was carried out for the label-free quantification process. The mass spectrometer was operated so that a 50-ms survey scan (TOF-MS) was performed and subsequent MS/MS experiments were performed on all precursors. These MS/MS experiments were carried out in a cyclical manner using an accumulation time of 40 ms per 25-Da swath (36 swaths in total) for a total cycle time of 1.5408 s. The ions were fragmented for each MS/MS experiment in the collision cell using the rolling collision energy. The MS data were acquired with Analyst TF

1.7 (AB SCIEX, Concord, Canada). Peptides (and proteins) were identified using DDA followed by database search, while the quantification was obtained by integrating the area under the chromatographic peak for each ion fragment of identified peptides by using the DIA file [23].

Spectral library generation and quantification

The DDA files were searched against the UniProt Swiss-Prot reviewed database containing human proteins (version 01.02.2018, containing 42,271 sequence entries) using Protein Pilot software v. 4.2 (SCIEX, Concord, Canada) and Mascot v. 2.4 (Matrix Science Inc., Boston, USA). Samples were put as input in the Protein Pilot software with the following parameters: cysteine alkylation, digestion by trypsin, no special factors and False Discovery Rate (FDR) at 1%. For Mascot search, we selected Trypsin as digestion enzyme with 2 missed cleavages, set the instrument to ESI-QUAD-TOF and specified the following modifications for the assay: carbamidomethyl cysteine as fixed modification and oxidized methionine as variable modification. An assay tolerance of 50 ppm was specified for peptide mass tolerance, and 0.1 Da for MS/MS tolerance. The charges of the peptides to search for were set to 2 +, 3 + and 4 +, and the search was set to monoisotopic. A target-decoy database search was performed, and FDR was fixed at 1%. SwathXtend was employed to build an integrated assay library with the DDA acquisitions to use as the ion library file for all SWATH analysis and quantification.

Quantification was performed by integrating the extracted ion chromatogram of all the unique ions for a given peptide. Spectral alignment of the SWATH samples (DIA run) was carried out with PeakView 2.2 (ABSCIEX, Concord, Canada) using the spectral library generated above and the following parameters: 6 peptides per protein, 6 transitions per peptide, XIC extraction window of 5 min and a width of 15 ppm. Shared peptides were excluded as well as peptides with modifications. Peptides with FDR lower than 1.0% were exported in MarkerView 1.2 (ABSCIEX, Concord, Canada) for the t-test [24]. The mass spectrometry proteomics data have been deposited in an internal repository at our institution.

Functional enrichment analysis of DEPs

Functional Enrichment analysis was performed using the R interface of the clusterProfiler package available in Bioconductor (version 3.21) [25]. The libraries considered for the functional analysis were GO Biological Process and GO Molecular Function. The genes codifying for the differentially expressed proteins were used as input data, selecting proteins characterized by Fold change > 1.3 and < 0.75 (52 proteins, three proteins did not have valid gene IDs. The terms with p-value < 0.05 obtained after multiple testing correction by Bonferroni's method were considered as significantly enriched in the interrogated libraries.

Enzyme-linked immunosorbent assays (ELISA)

The level of human B2M, TF, CO4 and DCD proteins was quantified blinded in serum (EPIC) or plasma (MoMar) samples using the following ELISA kits: Cat# Ab181423 for B2M, Cat# Ab1108911 for TF, Cat# Ab108824 for CO4 (Abcam, UK), Cat# EKX-T5NSZG-96 for DCD (Nordic BioSite, Denmark). The assays were performed according to the manufacturer's instructions, with the following sample dilutions (as determined by internal trials when not indicated in the kit instructions): B2M serum 1:400; B2M plasma 1:3200; CO4 serum 1:400; CO4 plasma 1:400; DCD serum 1:16; TF serum 1:2000; TF plasma 1:4000. The measurements of serum calretinin and mesothelin were determined by ELISA assays in the EPIC samples using the Calretinin ELISA kit (DLD Diagnostika, Hamburg, Germany) and Human Mesothelin ELISA kit (R&D systems Inc.) as previously described [26]. In the MoMar samples, plasma calretinin was also determined by ELISA assay using the Calretinin ELISA kit (DLD Diagnostika, Hamburg, Germany), plasma mesothelin (SMRP) was measured with the Lumipulse G Mesothelin assays (Fujirebio, Tokyo, Japan) using the CLEIA analyzer LUMIPULSE G600II (Fujirebio), according to the manufacturers' instructions [26]. Standard curve analysis for EPIC serum samples and MoMar plasma samples were constructed using the linear and 4-parameter logistic fit respectively as it was the most efficient setting to include the points at the low and high end of the curve.

Statistical analyses

All statistical analyses were conducted using the open source software R (version 4.2.1). Differentially expressed proteins in the EPIC Cohort, obtained by SWATH LC-MS/MS technique, were tested by a multiple regression model (R GLM function), controlling for age at blood collection, sex and level of asbestos exposure (no exposure, low or high); the selection for markers of interest was based on fold change (outside the interval [0.75; 1.3]) and nominal p-value (<0.05). The markers that were further validated by ELISA assay were used to conduct t-tests, Pearson's correlation analyses and multiple regressions in pre-diagnostic cases with respect to controls in the EPIC Cohort (TTD of

Table 1 Baseline characteristics of pre-diagnostic PM cases and matched non-cancer controls in the EPIC cohort

	Cases	Non-Cancer controls
Number, n	21	21
Mean Age ± SD	58.4 ± 7.29	58.44 ± 7.35
Male/Female, n	18/3	18/3
Exposure, n (frequency)		
No Exposure	4 (19%)	4 (19%)
Low	8 (38%)	8 (38%)
High	9 (43%)	9 (43%)
Time to Diagnosis(TTD) (Years) - Mean / SD	2.4/ 1.38	
Interval, n (frequency)		
0–2 years	10 (48%)	
2–5 years	11 (52%)	

Demographics include mean age (±SD) and sex distribution. Asbestos exposure is categorized as none, low, or high grade. Time to diagnosis (TTD) represents years from blood draw to clinical diagnosis (mean, SD). Cases are further stratified by TTD interval (0–2 years, 2–5 years) with corresponding frequencies

2 years or 2–5 years) and in the MoMar replication cohort (TTD < 1 year). ROC curve analyses were then employed in both the cohorts in order to evaluate the improvement in discrimination between pre-diagnostic PM and controls when adding the significant biomarkers to a base initial discrimination model including B2M protein (ROCR and pROC R packages), excluding matching variables (age, sex and exposure).

Results

Study population

The EPIC discovery cohort comprised 21 pre-clinical individuals who developed pleural mesothelioma (PM) within five years and 21 asbestos-exposed controls who remained disease-free over the same interval. Both groups were well matched for demographic and asbestos-exposure characteristics: the mean age was 58.4 ± 7.3 years in pre-clinical cases versus 58.4 ± 7.4 years in controls. Asbestos exposure levels were similarly distributed, with 19% reporting no known exposure, 38% low exposure, and 43% high exposure in both cases and controls.

Among the pre-clinical cases who developed PM, the average time from blood draw to clinical diagnosis was 2.4 ± 1.4 years. Nearly half of cases (48%) were diagnosed within two years of sampling, while the remaining 52% were diagnosed between two and five years later.

The baseline characteristics of the participants and the experimental setup of the study are displayed in Table 1; Fig. 1.

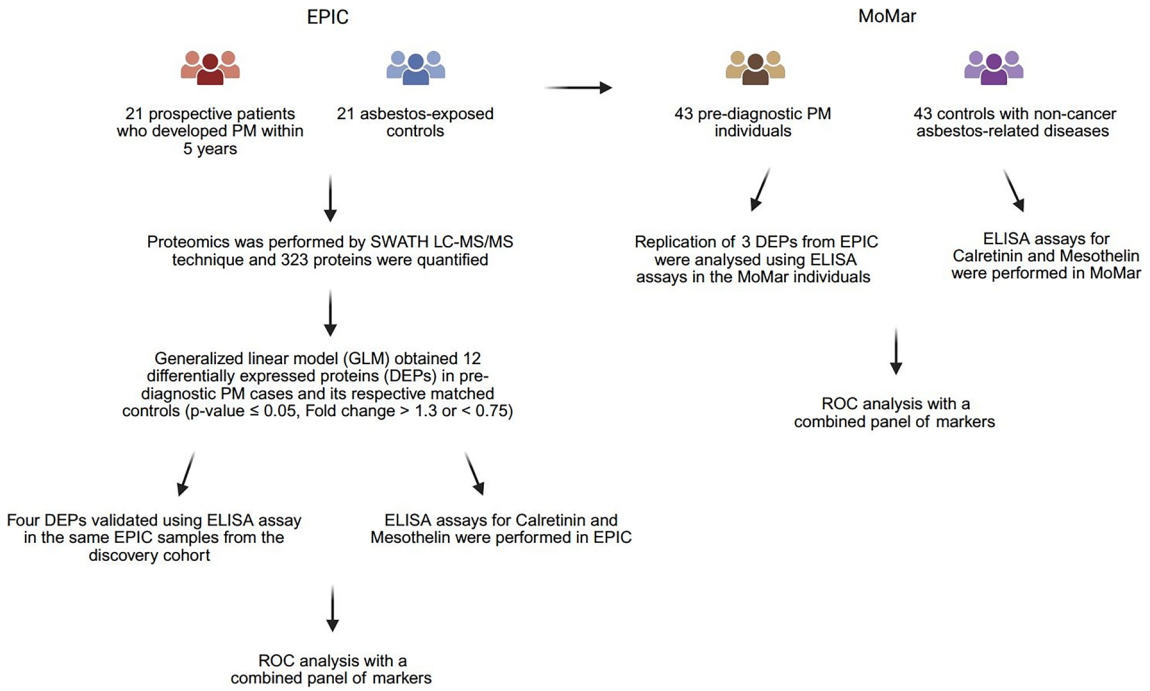

Fig. 1 Proteomics Workflow in EPIC and MoMar Cohorts. Left (EPIC): SWATH LC-MS/MS profiled 323 plasma proteins from 21 asbestos-exposed cases (PM within 5 years) and 21 matched controls. A GLM identified 12 DEPs ($p \leq 0.05$, fold change $\geq 1.3 \leq 0.75$); four were ELISA-validated. Calretinin and mesothelin benchmark ELISA assays were performed. Combined markers underwent ROC analysis Right (MoMar): Three DEPs from EPIC were quantified by ELISA alongside calretinin and mesothelin. ROC analysis of the combined protein panel assessed reproducibility and predictive accuracy in the pre-diagnosis cohort

Table 2 Differentially expressed proteins identified by generalized linear model in pre-diagnostic PM Sera

Protein ID	UniProt entry	Gene name	Protein name	Mean_cases	Mean_controls	*p*-value	FC
TF	P02787	*TF*	Transferrin	900329.95	628733.07	0.008	1.43
CO4A	P0C0L4	*CO4*	Complement C4-A	1143125.73	817472.39	0.009	1.40
B2MG	P61769	*B2M*	Beta-2-microglobulin	78389.73	106166.28	0.035	0.74
IGLL1	P15814	*IGLL1*	Immunoglobulin lambda-like polypeptide 1 (CD179b)	225090.02	307226.08	0.042	0.73
PHLD	P80108	*GPLD1*	Phosphatidylinositol-glycan-specific phospholipase D	61371.62	84574.80	0.026	0.73
IGLC3	P0DOY3	*IGLC3*	Immunoglobulin lambda constant 3	1069195.63	1505007.19	0.006	0.71
IGL1	P0DOX8		Immunoglobulin lambda-1 light chain	446957.84	674012.11	0.020	0.66
MAST2	Q6P0Q8	*MAST2*	Microtubule-associated serine/threonine-protein kinase 2	21040.46	31315.69	0.054	0.67
LV325	P01717	*IGLV3-25*	Immunoglobulin lambda variable 3–25	54779.20	85143.21	0.012	0.64
DCD	P81605	*DCD*	Dermcidin	6912.96	10933.02	0.029	0.63
F217A	Q8IXS0	*FAM217A*	Protein FAM217A	10299.09	20247.61	0.029	0.51
TM156	Q8N614	*TMEM156*	Transmembrane protein 156	26167.84	79165.85	0.045	0.33

FC: fold change (cases/controls); p-value: nominal significance from GLM were calculated in the EPIC cohort

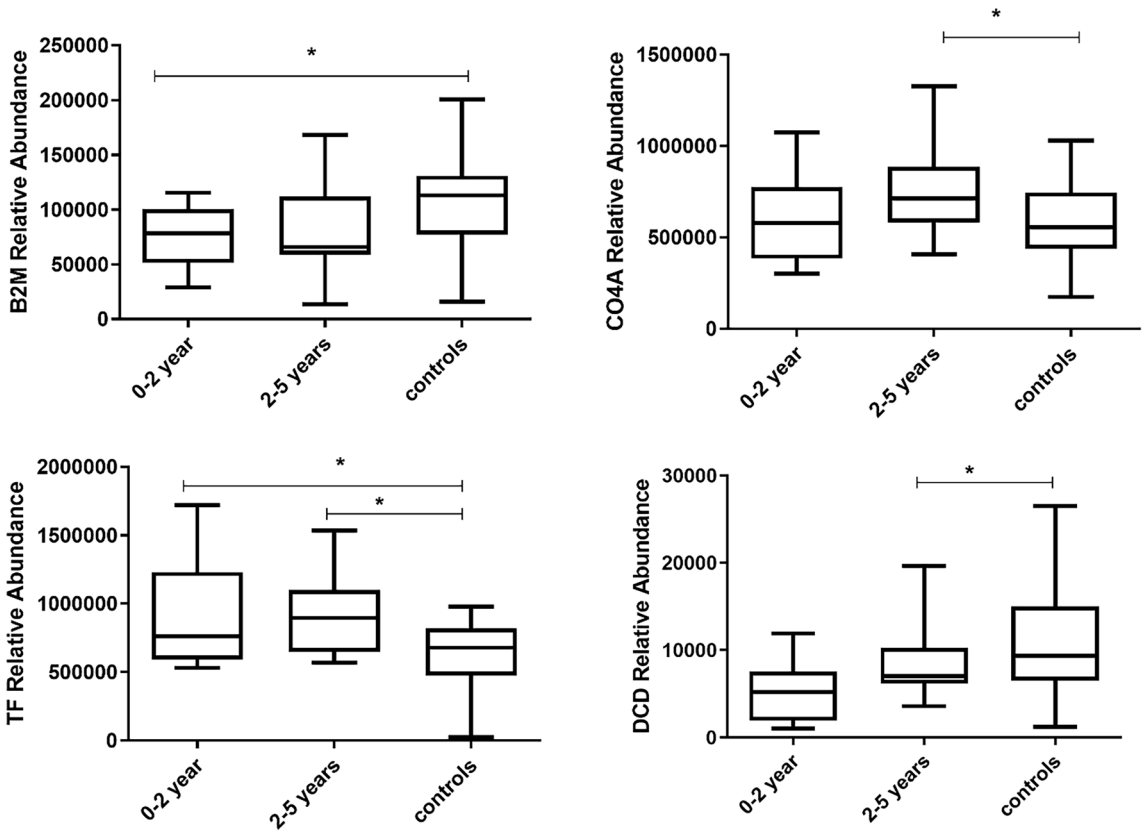

Fig. 2 Differential relative abundance of top serum proteins in pre-diagnostic PM cases versus controls. Box plots show relative LC-MS/MS intensities for each DEP grouped by time to diagnosis (0–2 years, 2–5 years) and matched controls. Up-regulated proteins include Complement C4A (C4; FC = 1.4, $p = 0.009$) and Transferrin (TF; FC = 1.4, $p = 0.008$). Down-regulated proteins comprise Beta-2-Microglobulin (B2M; FC = 0.7, $p = 0.035$), and Dermcidin (DCD; FC = 0.6, $p = 0.029$). Asterisks indicate nominal $p < 0.05$ by GLM

Differential proteomic signature in Pre-diagnostic PM Sera in the EPIC cohort

Proteomic profiling of pre-diagnostic EPIC sera versus matched controls quantified 323 proteins by LC-MS/MS. Using a fold-change threshold alone (FC > 1.3 or < 0.75), 55 proteins were differentially expressed: 17 up-regulated and 38 down-regulated (Table S1). A generalized linear model incorporating both magnitude (FC > 1.3 or < 0.75) and statistical significance (nominal $p < 0.05$) narrowed this list to 12 DEPs (Table 2; Fig. 2).

Among the up-regulated markers, complement C4 (C4, FC = 1.4, p-value = 0.009, FDR = 0.62) and transferrin (TF, FC = 1.4, p-value = 0.008, FDR = 0.62) exhibited elevated

levels in pre-diagnostic PM cases. Despite immunodepletion of high-abundance proteins, reproducible depletion across all samples validates TF as a true hit. Ten proteins were down-regulated, predominantly immunoglobulin family members including Immunoglobulin lambda-like polypeptide 1, CD179b (IGLL1), Immunoglobulin lambda constant 3 (IGLC3), Immunoglobulin lambda-1 light chain (IGL1), Immunoglobulin lambda variable 3–25 (IGLV3-25) as well as beta-2-microglobulin (B2M, FC = 0.7, p-value = 0.035) and dermcidin (DCD, FC = 0.6, p-value = 0.029), both previously implicated in cancer biology [27–30]. Box plots in Fig. 2 depict the relative abundance of these 12 DEPs across pre-clinical PM cases and controls.

Enrichment analysis and functional annotation of the deps

Functional enrichment analyses were performed to explore common biological processes regulated by the DEPs (FC > 1.3 and < 0.75) set in GO Biological Process and GO Molecular Function libraries (Supplementary fig. S1). The most significantly enriched pathways in GO Biological Process included wound healing, coagulation, hemostasis and regulation of body fluid levels ($p < 0.001$), collectively pointing to aberrant hemostatic activation prior to clinical diagnosis. Additional enriched processes encompassed complement activation (fibrinolysis, platelet activation) and immune regulation (negative regulation of coagulation, lymphocyte-mediated immunity) ($p < 0.05$).

Protein functional annotations were dominated by antigen binding ($p < 0.001$), glycosaminoglycan binding ($p < 0.01$), alongside multiple complement-related activities (complement binding, proteoglycan binding, serine-type endopeptidase activity). These findings suggest dysregulated extracellular matrix interactions, immune recognition processes, and proteolytic cascades in the pre-clinical phase.

Validation of Pre-diagnostic deps in EPIC cohort by ELISA

To validate the proteomic findings, four candidate proteins beta-2-microglobulin (B2M), transferrin (TF), complement C4 (C4), and dermcidin (DCD) were quantified by ELISA in the same pre-diagnostic EPIC samples and matched controls. These proteins were selected based on their established roles in tumor biology and inflammation.

All four DEPs were detectable in serum by ELISA and recapitulated the change of direction observed in SWATH LC-MS/MS. However, only B2M exhibited a borderline significant decrease in cases sampled 0–2 years before diagnosis compared to controls (t-test $p < 0.05$; GLM $p < 0.05$). TF, C4, and DCD trended similarly to discovery data but did not reach statistical significance. TTD subgroup analysis revealed that the B2M reduced levels was specific to cases within two years of diagnosis (t-test $p < 0.05$), whereas samples collected 2–5 years prior showed no significant difference from controls (t-test p-value = 0.26) (Fig. 3). Correlation analysis between proteomic and ELISA measurements demonstrated a modest but significant association for B2M (Pearson $r = 0.320$, $p = 0.04$), supporting its reproducible quantification across platforms.

Replication of candidate deps in the MoMar cohort

To assess reproducibility, ELISAs for B2M, TF, and C4 were performed on plasma from the MoMar replication cohort ($n = 86$). This set included 32 asbestos-exposed individuals sampled within one year before PM diagnosis (pre-diagnostic cases) and 32 age- and sex-matched controls with non-cancer asbestos-related conditions (Table 3). None of the three proteins showed significant differences between pre-diagnostic cases and controls (Fig. 4).

Calretinin and mesothelin profiling in Pre-diagnostic EPIC and MoMar samples

Calretinin and mesothelin, key immunohistochemical markers in PM diagnosis, were quantified by ELISA to evaluate their blood-based diagnostic potential. A combined plasma panel of these markers previously detected 44% of mesothelioma cases at 98% specificity in pre-diagnostic samples [31]. In the MoMar cohort, calretinin levels in plasma collected 0–2 years before diagnosis were markedly elevated in pre-diagnostic cases versus non-cancer controls ($p < 0.01$). In contrast, calretinin in EPIC serum samples during the same interval showed only a modest, non-significant increase (Fig. 4). Mesothelin concentrations rose in the 0–2 years window in both cohorts but achieved statistical significance only in MoMar ($p < 0.0001$) (Fig. 5). Subdividing MoMar cases into one-year intervals (Table 3) revealed peak marker elevations within 0–1 year pre-diagnosis group using established thresholds (calretinin ≥ 0.6 ng/mL; mesothelin ≥ 2.26 nM), as shown in Supplementary Figure S2.

Combined biomarker panel from EPIC and MoMar enhances Pre-diagnostic PM detection

To evaluate the risk-discriminatory power, a generalized linear model (GLM) combination of five markers B2M, TF, C4, Calretinin, and Mesothelin was considered in pre-diagnostic cases sampled < 2 years before diagnosis across both EPIC and MoMar cohorts. In the MoMar cohort, the full five-marker panel achieved an AUC of 0.91 (p-value = 0.001), driven primarily by calretinin and mesothelin contributions

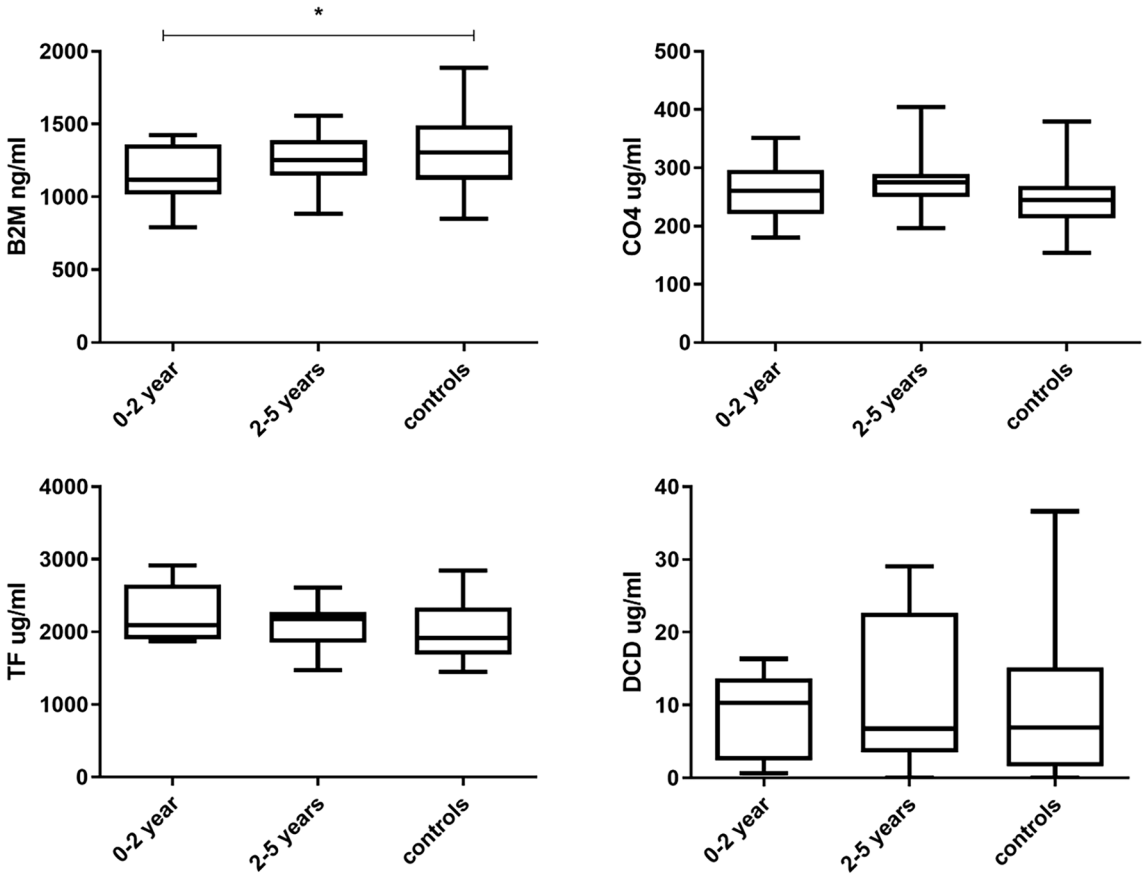

Fig. 3 ELISA validation of candidate DEPs in pre-diagnostic EPIC sera. Box plots display serum concentrations of B2M (ng/mL), C4 (µg/mL), TF (µg/mL), and DCD (µg/mL) in cases sampled 0–2 years and 2–5 years before PM diagnosis versus matched controls. B2M showed a borderline significant increase in the 0–2 year group (t-test and GLM $p<0.05$); TF, C4, and DCD trended similarly but were not significant. Asterisks indicate nominal $p<0.05$

Table 3 Baseline characteristics of pre-diagnostic PM cases and matched non-cancer controls in the MoMar cohort

	Cases	Non-Cancer controls
Number, n	43	43
Mean Age ± SD	74 ± 4.85	74 ± 4.95
Male/Female, n	43/0	43/0
Time to Diagnosis, years - Mean / SD	0.8/ 0.73	
Interval, n (frequency)		
> 0–1 years	32 (74%)	
> 1–2 years	7 (16%)	
> 2–3 years	3 (7%)	
> 3–4 years	1 (2%)	
> 4–5 years	0	

Demographics include number, mean age (±SD), and sex distribution. Time to diagnosis (TTD) indicates years from blood draw to clinical diagnosis (mean ± SD). Cases are further stratified by TTD intervals (> 0–1, > 1–2, > 2–3, > 3–4, > 4–5 years) with corresponding frequencies

(Fig. 6B). In EPIC, the same panel yielded an AUC of 0.88 (p-value = 0.17), not significantly different from individual EPIC markers alone. By contrast, the three EPIC-derived proteins (B2M, C4, TF) assessed in isolation displayed lower discriminative power in both cohorts (Fig. 6A and B). These results demonstrate that integrating tumor-specific markers with potential proteomic biomarker candidates substantially improves early PM detection performance.

Discussion

Pleural mesothelioma (PM) remains a fatal malignancy driven by asbestos exposure, and its long latency and non-specific early symptoms has been a hindrance towards timely diagnosis and intervention. The absence of reliable pre-tumor biomarkers for risk stratification and early detection underscores an urgent clinical need. Over the past decade, blood proteomic profiling has emerged as a promising strategy for identifying early cancer signatures in high-risk cohorts [32]. We hypothesized that the most pronounced

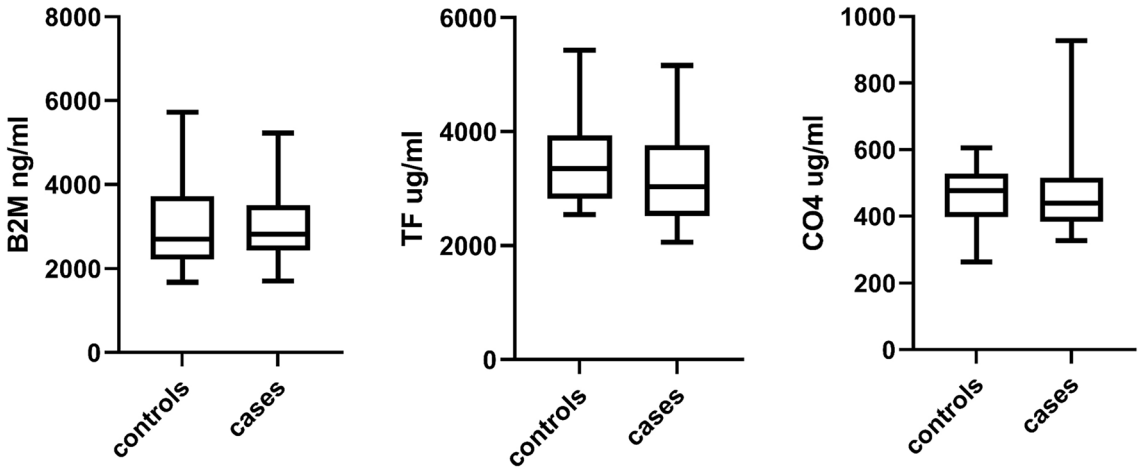

Fig. 4 ELISA replication of candidate DEPs in MoMar plasma. Box plots show concentrations of B2M (ng/mL), TF (µg/mL), and C4 (µg/mL) in pre-diagnostic cases versus asbestos-exposed non-cancer controls. No significant differences were observed for any marker

proteomic alterations would manifest in the years close to clinical diagnosis. Utilizing high-throughput SWATH-MS in the EPIC discovery cohort, we quantified 323 serum proteins and identified 55 candidates (FC > 1.3 or < 0.75), of which 12 remained statistically significant after applying GLM ($p < 0.05$). Subsequent ELISA validation in the discovery cohort confirmed reproducible trends for B2M, C4, TF, and DCD, although only B2M demonstrated a borderline significance and association in cases sampled within two years of diagnosis. The ELISA validation of proteins B2M, CO4 and TF were performed in the MoMar cohort but results couldn't be replicated, a limitation addressed later. B2M plays a central role in antigen presentation via the MHC class I complex. In the study by Mangiante et al., multi-omics profiling of PM tumors revealed that whole-genome doubling (WGD+) cases frequently downregulate B2M, leading to impaired immune surveillance and "cold" tumor phenotypes [7]. Our observation of decreased levels of circulating B2M shortly before diagnosis in the 0–2 TTD group represents a counterintuitive finding that divulges from the current established literature where B2M associates with tumor burden and poor prognosis across multiple malignancies [33]. PM's immunosuppressive tumor microenvironment, featuring regulatory T cell accumulation, and myeloid-derived suppressor cells, globally dampens systemic immune responses and the decreased B2M may reflect early immune evasion through HLA Class I downregulation rather than immune activation, characteristic of other tumors. Since B2M is a critical structural component of MHC Class I molecules, malignant cells that suppress HLA Class I expression would simultaneously reduce B2M synthesis and secretion [34–37]. This might represent a Phase 1 (pre-diagnostic) immune signature characterized by immune suppression during early malignant transformation, distinct from phase 2 (established PM) dynamics when secondary immune activation may normalize or increase B2M. The temporal clustering of B2M decrease specifically in the 0–2 years pre-diagnostic window with no significant difference at 2–5 years ($p = 0.26$) supports this phase-specific interpretation forming a distinct PM pre-diagnostic signature rather than representing a non-specific inflammation marker, and may capture PM-specific early immune suppression potentially enhancing panel specificity when combined with tumor-associated markers. Transferrin (TF) on the other hand mediates cellular iron uptake, and iron overload is implicated in asbestos-induced carcinogenesis through oxidative DNA damage and chronic inflammation. Although TF abundance trended higher in cases, serum levels did not reach significance, possibly due to biological variability and immuno-depletion effects [38, 39]. Complement component C4 was increased in cases 2–5 years before diagnosis, consistent with reports that complement subunits C4d and C1q correlate with tumor burden, chemotherapy resistance, and poor survival in PM. Aberrant complement activation may foster a pro-tumorigenic microenvironment through wound-healing pathways and immunomodulation [40, 41]. Dermcidin (DCD), a secreted antimicrobial peptide, has been implicated in tumor progression and invasion across several cancers was downregulated in pre-clinical sera suggesting a complex, context-dependent role in early PM pathogenesis that merits further mechanistic study.

Enrichment of complement binding and wound-healing pathways parallels reports that non-canonical C1q activation fosters mesothelioma cell adhesion and migration via hyaluronic acid interactions, while coagulation and platelet activation signatures reflect tumor-driven fibrin deposition and prothrombotic states that could foretell poor prognosis [42]. Concurrent downregulation of immunoglobulin family members and enrichment of lymphocyte-mediated immunity processes mirror the immunosuppressive, "cold" tumor

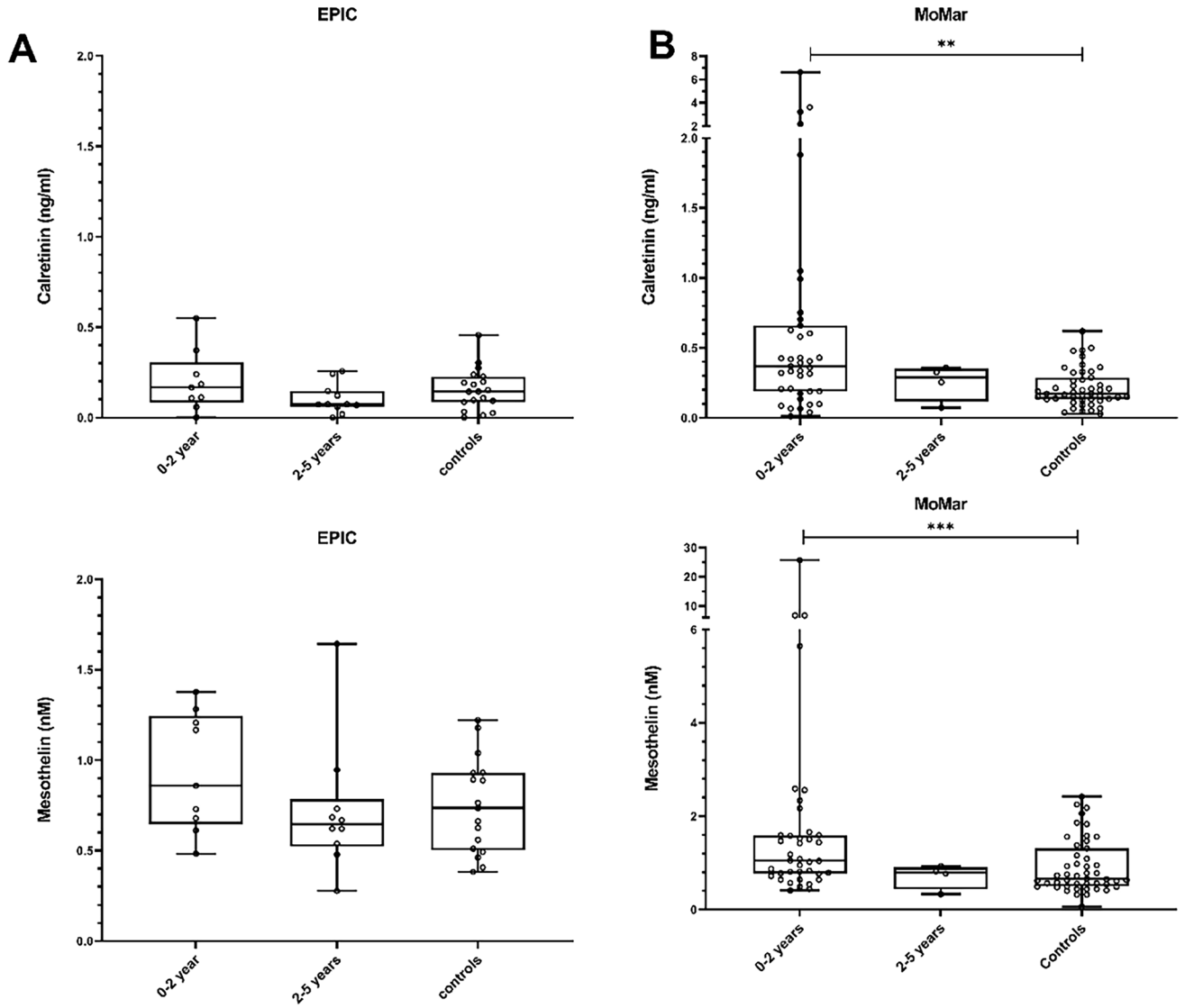

Fig. 5 ELISA quantification of calretinin and mesothelin in pre-diagnostic EPIC and MoMar samples. (**A**) EPIC serum: calretinin (ng/mL) and mesothelin (nM) levels in cases sampled 0–2 years and 2–5 years before diagnosis versus controls. (**B**) MoMar plasma: calretinin and mesothelin levels in 0–2 years and 2–5 years pre-diagnostic cases compared to asbestos-exposed non-cancer controls. Calretinin was significantly elevated in MoMar cases at 0–2 years ($p < 0.01$), whereas EPIC increases were not significant. Mesothelin levels reached significance only in MoMar ($p < 0.0001$). Asterisks indicate significance (** $p < 0.01$; *** $p < 0.0001$)

microenvironment in PM, characterized by exhausted T cells and regulatory macrophages, and suggest that early adaptive immune dysfunction is detectable in blood years before clinical diagnosis [43]. These enrichment patterns provide biological context for the observed proteomic changes and suggest that complement activation, hemostatic dysregulation, and immune microenvironment alterations are detectable years before PM diagnosis.

Calretinin and mesothelin, standard immunohistochemical markers for PM, demonstrated complementary performance in plasma. In the MoMar cohort, calretinin was highly elevated within one year of diagnosis, whereas serum measurements in EPIC showed only a modest increase. Mesothelin levels rose in both cohorts in the two-year window but achieved statistical significance only in plasma. While Calretinin and Mesothelin are PM-enriched they are not PM-exclusive. Immunohistochemical studies show calretinin expression in lung cancer with frequencies varying by histological subtype, approximately 15% of lung adenocarcinomas particularly in advanced-stage, smoker-associated tumors and in about 54% of squamous cell carcinomas [44]. Blood-based calretinin elevation occurs in mesothelioma and, at lower frequencies, in lung cancer, though systematic comparative data in a pre-diagnostic setting are limited. Lehnert et al. demonstrated that plasma calretinin intensity correlates with tumor tissue calretinin

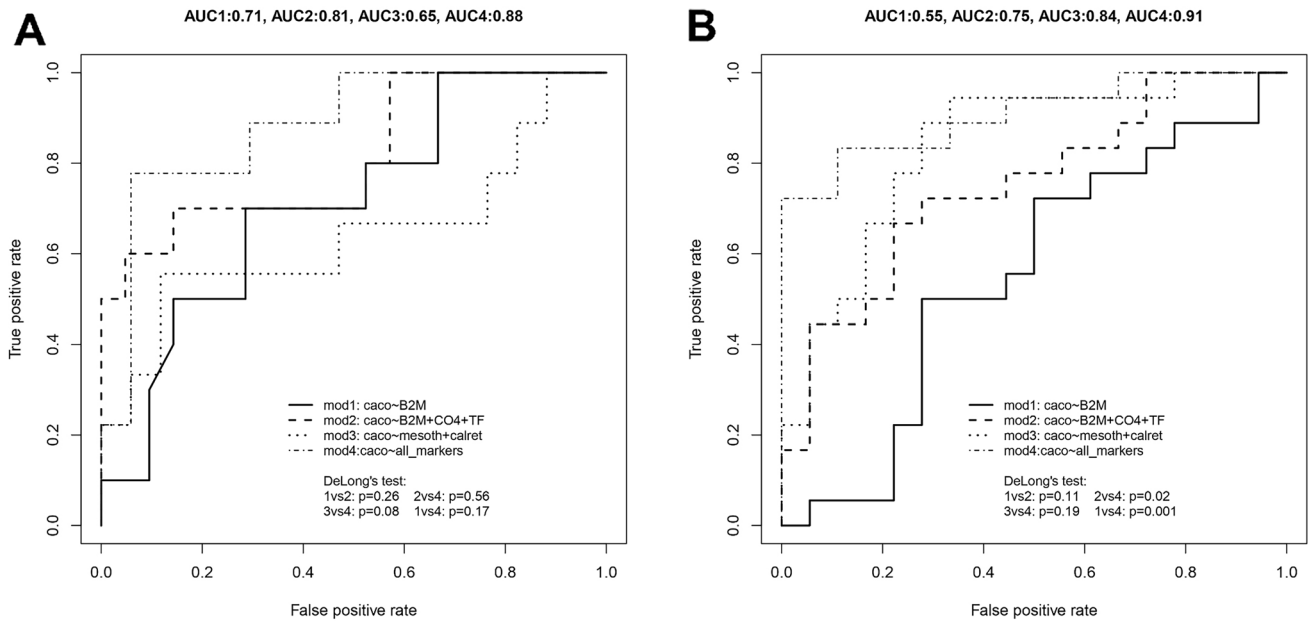

Fig. 6 Receiver operating characteristics (ROC) analysis of combined biomarker panels in pre-diagnostic PM cases. (**A**) EPIC cohort: ROC curves for models using B2M alone (mod1, AUC = 0.71), B2M + C4 + TF (mod2, AUC = 0.81), Mesothelin + Calretinin (mod3, AUC = 0.65), and all five markers (mod4, AUC = 0.88; p-value = 0.17 vs. mod1 by DeLong's test). (**B**) MoMar cohort: ROC curves for the same models (mod1 AUC = 0.55), mod2 (AUC = 0.75), mod3 (AUC = 0.84), and mod4 (AUC = 0.91; $p = 0.001$ vs. mod1)

immunohistochemical expression in mesothelioma patients, validating blood-based calretinin and its reflection at the PM tissue-level [45]. Our findings of elevated calretinin and mesothelin in pre-diagnostic PM aligns with previous prospective studies showing that calretinin and mesothelin levels tend to rise within a year prior to clinical detection. In the first prospective cohort study, Johnen et al. showed that calretinin and mesothelin increase predominantly in the year preceding clinical diagnosis, supporting their utility as pre-diagnostic screening markers in asbestos-exposed workers. At 95% specificity, calretinin achieved 71% sensitivity for mesothelioma detection; notably, the calretinin-mesothelin combination increased mesothelin sensitivity from 66% to 75%, demonstrating that multi-marker approaches enhance diagnostic accuracy [46]. Zupanc et al. further validated these findings in 549 subjects, confirming that serum calretinin achieved an AUC of 0.826 for mesothelioma prediction, with calretinin-mesothelin combination providing the highest predictive value [47].

These findings mirror prior additional works showing a combined plasma panel of calretinin and mesothelin in detecting PM cases and support their inclusion in surveillance programs for asbestos-exposed workers [48–50]. Nevertheless, direct evidence comparing blood calretinin and mesothelin levels between pre-diagnostic lung cancer and PM particularly among asbestos-exposed populations is lacking, representing a key limitation. Integrating EPIC and MoMar proteomic biomarker candidates, the five-protein GLM model achieved robust discrimination of pre-diagnostic PM (TTD < 2 years), with AUCs of 0.88 in EPIC and 0.91 in MoMar. This performance surpasses that of either the EPIC (B2M, C4, TF) or MoMar (calretinin, mesothelin) marker sets alone, underscoring the value of combining inflammation/immune dysregulation and tumor-associated markers for early detection.

Despite limited individual marker specificity, the combined multi-marker panel, within the specific context of PM surveillance would be clinically relevant, allowing for timely intervention and implementation of more effective treatments. Risk stratification in high-risk cohorts represents the primary application: in asbestos-exposed workers with documented occupational exposure and benign asbestos-related disease, elevated calretinin and mesothelin particularly within one year of baseline examination could trigger intensified CT surveillance protocols, potentially enabling earlier mesothelioma detection when curative surgery remains feasible. Our five-marker panel (calretinin, mesothelin, B2M, transferrin, complement C4) achieved AUC values of 0.91 (MoMar) and 0.88 (EPIC), demonstrating that combining PM-associated markers with systemic inflammation/immune markers improves discrimination over individual biomarkers alone. This integrated approach captures both direct tumor-derived signals (calretinin, mesothelin) and tumor inflammatory/immune-related signatures (B2M, C4, transferrin), providing a more comprehensive immunobiological profile. Longitudinal monitoring rather than single-threshold assessment may enhance specificity especially in asbestos-exposed workers undergoing

serial occupational health examinations, rising trends in multi-marker values over time rather than static thresholds could provide more specific early warning signals. Clinical integration of biomarkers with imaging and exposure data substantially strengthens predictive utility. Rather than biomarker interpretation in isolation, a comprehensive risk assessment combining elevated multi-marker panel results with high-resolution CT findings (pleural thickening, nodules), quantified occupational asbestos exposure intensity, and emerging genetic risk scores could generate robust personalized risk prediction models for mesothelioma surveillance programs. This kind of a multi-modal approach leverages the complementary strengths of molecular, radiological, occupational, and genetic information for enhanced early detection in asbestos-exposed populations.

Conclusion

In conclusion, our multi-cohort proteomic approach identifies a novel composite biomarker panel that enhances early PM risk discrimination among asbestos-exposed individuals. The identification of decreased pre-diagnostic B2M as a potential PM-specific immune suppression signature represents a novel finding warranting further mechanistic investigation. The five-marker panel outperforms individual markers and captures complementary tumor-derived and microenvironment signals. Validation in larger, diverse prospective cohorts and integration with imaging data or genetic risk factors could pave the way towards pre-symptomatic detection and improved patient outcomes.

Limitations

Taken together, both EPIC and MoMar represent prospective cohorts with pre-diagnostic sampling, while providing temporal advantages over purely retrospective studies and should be acknowledged when interpreting biomarker performance. The lack of ELISA marker reproducibility observed in MoMar, despite employing identical assay platforms likely reflects multiple identifiable inter-cohort differences. First, MoMar controls had confirmed benign asbestos-related pulmonary diseases (asbestosis, pleural plaques) representing chronic inflammatory states, whereas EPIC controls were subjects who had varying asbestos-exposure grades but were clinically healthy. Since C4 and TF are elevated in chronic inflammation, this comparison might have narrowed detectable differences for markers elevated in both pre-diagnostic cases and diseased controls due to shared inflammatory pathology. Second, biospecimen matrix differences - EPIC serum versus MoMar plasma, affect protein stability, and ELISA performance can be different especially for complement proteins and acute-phase reactants. Third, varying temporal sampling patterns: 74% of MoMar cases were sampled within one year of diagnosis compared to a broader 0-5-year distribution in EPIC. The compressed MoMar sampling window may reduce statistical power while preventing assessment of longer-timeframe markers. Fourth, it was not possible to account for renal function, a major confounder for B2M that couldn't be systematically measured. Fifth, MoMar controls showed higher baseline calretinin and mesothelin levels than EPIC controls, likely reflecting chronic mesothelial stimulation from benign asbestos-related disease, thereby reducing protein abundance discrimination. Collectively, these factors, diseased controls with baseline inflammation, matrix differences, compressed temporal sampling, unmeasured renal function confounding, and elevated marker baselines could explain the reproducibility challenges and prevent detection of the biomarkers observed in EPIC [51]. These limitations underscore the need for biomarker validation by paying careful attention to cohort characteristics, temporal sampling strategies and larger multi center efforts are required before clinical implementation.

Supplementary Information The online version contains supplementary material available at https://doi.org/10.1007/s10238-026-02058-x.

Acknowledgements We would like to acknowledge the involvement of the National Institute for Public Health and the Environment (RIVM), Bilthoven, the Netherlands, for their contribution and ongoing support to the EPIC Study.We would also like to thank our fellow lab colleagues especially for their unwavering support during the course of this work.

Author contributions EJH - Conceptualization, methodology, investigation, formal analysis, visualization, validation, writing – original draft, project administration AA - Conceptualization, methodology, investigation, formal analysis, software, visualization, validation, writing – original draft, project administration CV - Data curation, software, formal analysis, writing – original draft MM - Methodology, data curation, resources, formal analysis AR - Data curation, writing – review & editing KSH - Data curation, writing – review & editing NK - Methodology, investigation, formal analysis, writing – original draft, validation, visualization, resourcesGJ - Methodology, investigation, formal analysis, writing – original draft, validation, visualization, resources TB - Data curation, writing – review & editing DM - Data curation, writing – review & editing ID - Data curation, writing – review & editing AA (Antonio Agudo) - Data curation, writing – review & editing EW - Data curation, resources, writing – review & editing VS - Data curation, writing – review & editing RK - Data curation, resources, writing – review & editing RTF - Data curation, writing – review & editing RT - Data curation, writing – review & editing LM - Data curation, writing – review & editing JMGN - Data curation, resources, writing – review & editing MBS - Data curation, resources, writing – review & editing CS - Data curation, resources, writing – review & editing NCC - Data curation, resources, writing – review & editing GM (Giovanna Masala) - Data curation, writing – review & editing MG - Data curation, writing – review & editing PV - Conceptualization EC - Conceptualization, supervision, project administration

GM - Conceptualization, supervision, project administratio, writing – review & editing. All authors read, edited, gave valuable feedbacks and revised the manuscript.

Funding information The research leading to these results has received funding from AIRC under IG 2018 - ID. 21390 project – P.I. Matullo Giuseppe and from the Ministero dell'Istruzione, dell'Università e della Ricerca—c (n° D15D18000410001, to G.M.) to the Department of Medical Sciences, University of Turin.

Data availability Raw mass spectrometry data generated in this study will be available through the EPIC central database (IARC/WHO). Access to the EPIC data is governed by the EPIC access policy, as detailed in https://epic.iarc.fr/access/. Please contact the corresponding author Giuseppe Matullo for more information.

Declarations

Competing interests The Institute for Prevention and Occupational Medicine of the German Social Accident Insurance (IPA) has supplied DLD Diagnostika GmbH with the antibodies to produce the Calretinin ELISA kits. In turn, the IPA has received Calretinin ELISA kits at a reduced price and may benefit from future sales of the kits. Otherwise, the individual authors declare no competing interests.

Ethics statement The study was approved by the Institutional Review Board of IARC and the ethics committees in the participating countries. All participants gave their written informed consent to participate in the EPIC study. The present study was carried out in accordance with the ethical principles of the Declaration of Helsinki.

Consent for publication Not applicable.

References

1. Kindler HL, Ismaila N, Bazhenova L, Chu Q, Churpek JE, Dagogo-Jack I, et al. Treatment of pleural mesothelioma: ASCO guideline update. J Clin Oncol. 2025;43(8):1006–38.
2. Robinson BW, Musk AW, Lake RA. Malignant mesothelioma. Lancet. 2005;366(9483):397–408.
3. Janes SM, Alrifai D, Fennell DA. Perspectives on the treatment of malignant pleural mesothelioma. N Engl J Med. 2021;385(13):1207–18.
4. Laaksonen S, Kettunen E, Sutinen E, Ilonen I, Vehmas T, Tormakangas T, et al. Pulmonary asbestos fiber burden is related to patient survival in malignant pleural mesothelioma. J Thorac Oncol. 2022;17(8):1032–41.
5. Hmeljak J, Sanchez-Vega F, Hoadley KA, Shih J, Stewart C, Heiman D, et al. Integrative molecular characterization of malignant pleural mesothelioma. Cancer Discov. 2018;8(12):1548–65.
6. Bueno R, Stawiski EW, Goldstein LD, Durinck S, De Rienzo A, Modrusan Z, et al. Comprehensive genomic analysis of malignant pleural mesothelioma identifies recurrent mutations, gene fusions and splicing alterations. Nat Genet. 2016;48(4):407–16.
7. Mangiante L, Alcala N, Sexton-Oates A, Di Genova A, Gonzalez-Perez A, Khandekar A, et al. Multiomic analysis of malignant pleural mesothelioma identifies molecular axes and specialized tumor profiles driving intertumor heterogeneity. Nat Genet. 2023;55(4):607–18.
8. Schmid S, Holer L, Gysel K, Koster KL, Rothschild SI, Boos LA, et al. Real-World outcomes of patients with malignant pleural mesothelioma receiving a combination of ipilimumab and nivolumab as First- or Later-Line treatment. JTO Clin Res Rep. 2024;5(12):100735.
9. Pass HI, Alimi M, Carbone M, Yang H, Goparaju CM. Mesothelioma biomarkers: A review highlighting contributions from the early detection research network. Cancer Epidemiol Biomarkers Prev. 2020;29(12):2524–40.
10. Sekido Y. Molecular pathogenesis of malignant mesothelioma. Carcinogenesis. 2013;34(7):1413–9.
11. Wulfkuhle JD, Liotta LA, Petricoin EF. Proteomic applications for the early detection of cancer. Nat Rev Cancer. 2003;3(4):267–75.
12. Hanash S, Taguchi A. Application of proteomics to cancer early detection. Cancer J. 2011;17(6):423–8.
13. Allione A, Viberti C, Cotellessa I, Catalano C, Casalone E, Cugliari G, et al. Blood cell DNA methylation biomarkers in preclinical malignant pleural mesothelioma: the EPIC prospective cohort. Int J Cancer. 2023;152(4):725–37.
14. Ostroff RM, Mehan MR, Stewart A, Ayers D, Brody EN, Williams SA, et al. Early detection of malignant pleural mesothelioma in asbestos-exposed individuals with a noninvasive proteomics-based surveillance tool. PLoS ONE. 2012;7(10):e46091.
15. Pesch B, Bruning T, Johnen G, Casjens S, Bonberg N, Taeger D, et al. Biomarker research with prospective study designs for the early detection of cancer. Biochim Biophys Acta. 2014;1844(5):874–83.
16. Suhre K, McCarthy MI, Schwenk JM. Genetics Meets proteomics: perspectives for large population-based studies. Nat Rev Genet. 2021;22(1):19–37.
17. Alvez MB, Edfors F, von Feilitzen K, Zwahlen M, Mardinoglu A, Edqvist PH, et al. Next generation pan-cancer blood proteome profiling using proximity extension assay. Nat Commun. 2023;14(1):4308.
18. Riboli E, Hunt KJ, Slimani N, Ferrari P, Norat T, Fahey M, et al. European prospective investigation into cancer and nutrition (EPIC): study populations and data collection. Public Health Nutr. 2002;5(6B):1113–24.
19. Riboli E, Kaaks R. The EPIC project: rationale and study design. European prospective investigation into cancer and nutrition. Int J Epidemiol. 1997;26(Suppl 1):S6–14.
20. Weber DG, Casjens S, Wichert K, Lehnert M, Taeger D, Rihs HP et al. Tasks and experiences of the Prospective, Longitudinal, multicenter MoMar (Molecular Markers) study for the early detection of mesothelioma in individuals formerly exposed to asbestos using liquid biopsies. Cancers (Basel). 2023;15(24):5896.
21. Taeger D, Wichert K, Lehnert M, Casjens S, Pesch B, Weber DG, et al. Lung cancer and mesothelioma risks in a prospective cohort of workers with asbestos-related lung or pleural diseases. Am J Ind Med. 2022;65(8):652–9.
22. Casalone E, Birolo G, Pardini B, Allione A, Russo A, Catalano C et al. Serum extracellular Vesicle-Derived MicroRNAs as

potential biomarkers for pleural mesothelioma in a European prospective study. Cancers (Basel). 2022;15(1):125.
23. Manfredi M, Conte E, Barberis E, Buzzi A, Robotti E, Caneparo V, et al. Integrated serum proteins and fatty acids analysis for putative biomarker discovery in inflammatory bowel disease. J Proteom. 2019;195:138–49.
24. Martinotti S, Patrone M, Manfredi M, Gosetti F, Pedrazzi M, Marengo E, et al. HMGB1 Osteo-Modulatory action on osteosarcoma SaOS-2 cell line: an integrated study from biochemical and -Omics approaches. J Cell Biochem. 2016;117(11):2559–69.
25. Yu G, Wang LG, Han Y, He QY. ClusterProfiler: an R package for comparing biological themes among gene clusters. OMICS. 2012;16(5):284–7.
26. Casjens S, Johnen G, Raiko I, Pesch B, Taeger D, Topfer C, et al. Re-evaluation of potential predictors of calretinin and mesothelin in a population-based cohort study using assays for the routine application in clinical medicine. BMJ Open. 2021;11(2):e039079.
27. Wang H, Liu B, Wei J. Beta2-microglobulin(B2M) in cancer immunotherapies: biological function, resistance and remedy. Cancer Lett. 2021;517:96–104.
28. Roumenina LT, Daugan MV, Petitprez F, Sautes-Fridman C, Fridman WH. Context-dependent roles of complement in cancer. Nat Rev Cancer. 2019;19(12):698–715.
29. Stewart GD, Skipworth RJ, Pennington CJ, Lowrie AG, Deans DA, Edwards DR, et al. Variation in Dermcidin expression in a range of primary human tumours and in hypoxic/oxidatively stressed human cell lines. Br J Cancer. 2008;99(1):126–32.
30. Zhao J, Peng H, Gao J, Nong A, Hua H, Yang S, et al. Current insights into the expression and functions of tumor-derived Immunoglobulins. Cell Death Discov. 2021;7(1):148.
31. Johnen G, Burek K, Raiko I, Wichert K, Pesch B, Weber DG, et al. Prediagnostic detection of mesothelioma by Circulating calretinin and mesothelin - a case-control comparison nested into a prospective cohort of asbestos-exposed workers. Sci Rep. 2018;8(1):14321.
32. Zafar S, Hafeez A, Shah H, Mutiullah I, Ali A, Khan K, et al. Emerging biomarkers for early cancer detection and diagnosis: challenges, innovations, and clinical perspectives. Eur J Med Res. 2025;30(1):760.
33. Prizment AE, Linabery AM, Lutsey PL, Selvin E, Nelson HH, Folsom AR, et al. Circulating Beta-2 microglobulin and risk of cancer: the atherosclerosis risk in communities study (ARIC). Cancer Epidemiol Biomarkers Prev. 2016;25(4):657–64.
34. Perarnau B, Siegrist CA, Gillet A, Vincent C, Kimura S, Lemonnier FA. Beta 2-microglobulin restriction of antigen presentation. Nature. 1990;346(6286):751–4.
35. Berko D, Carmi Y, Cafri G, Ben-Zaken S, Sheikhet HM, Tzehoval E, et al. Membrane-anchored beta 2-microglobulin stabilizes a highly receptive state of MHC class I molecules. J Immunol. 2005;174(4):2116–23.
36. Dhatchinamoorthy K, Colbert JD, Rock KL. Cancer immune evasion through loss of MHC class I antigen presentation. Front Immunol. 2021;12:636568.
37. Okita R, Mimura-Kimura Y, Kawamoto N, Yamamoto N, Umeda M, Okada M, et al. Effects of tumor-infiltrating CD8+T cells, PD1/PD-L1 axis, and expression patterns of HLA class I on the prognosis of patients with malignant pleural mesothelioma who underwent extra-pleural pneumonectomy. Cancer Immunol Immunother. 2023;72(4):865–79.
38. Toyokuni S. Iron overload as a major targetable pathogenesis of asbestos-induced mesothelial carcinogenesis. Redox Rep. 2014;19(1):1–7.
39. Jiang L, Akatsuka S, Nagai H, Chew SH, Ohara H, Okazaki Y, et al. Iron overload signature in chrysotile-induced malignant mesothelioma. J Pathol. 2012;228(3):366–77.
40. Klikovits T et al. Nov. Circulating complement component 4d (C4d) correlates with tumor volume, chemotherapeutic response and survival in patients with malignant pleural mesothelioma. Scientific reports vol. 7,1 16456. 28 2017, https://doi.org/10.1038/s41598-017-16551-7
41. Agostinis C et al. Nov. Complement Protein C1q Binds to Hyaluronic Acid in the Malignant Pleural Mesothelioma Microenvironment and Promotes Tumor Growth. *Frontiers in immunology* vol. 8 1559. 20 2017, https://doi.org/10.3389/fimmu.2017.01559
42. Rouka E, Beltsios E, Goundaroulis D, Vavougios GD, Solenov EI, Hatzoglou C et al. In Silico transcriptomic analysis of Wound-Healing-Associated genes in malignant pleural mesothelioma. Med (Kaunas). 2019;55(6):267.
43. Harber J, Kamata T, Pritchard C, Fennell D. Matter of TIME: the tumor-immune microenvironment of mesothelioma and implications for checkpoint Blockade efficacy. J Immunother Cancer. 2021;9(9):e003032.
44. Matsuda M, Ninomiya H, Wakejima R, Inamura K, Okumura S, Mun M, et al. Calretinin-expressing lung adenocarcinoma: distinct characteristics of advanced stages, smoker-type features, and rare expression of other mesothelial markers are useful to differentiate epithelioid mesothelioma. Pathol Res Pract. 2020;216(3):152817.
45. Lehnert M, Weber DG, Taeger D, Raiko I, Kollmeier J, Stephan-Falkenau S, et al. Determinants of plasma calretinin in patients with malignant pleural mesothelioma. BMC Res Notes. 2020;13(1):359.
46. Johnen G, Gawrych K, Raiko I, Casjens S, Pesch B, Weber DG, et al. Calretinin as a blood-based biomarker for mesothelioma. BMC Cancer. 2017;17(1):386.
47. Zupanc C, Franko A, Strbac D, Dodic Fikfak M, Kovac V, Dolzan V et al. Serum calretinin as a biomarker in malignant mesothelioma. J Clin Med. 2021;10(21):4875.
48. Casjens S, Weber DG, Johnen G, Raiko I, Taeger D, Meinig C, et al. Assessment of potential predictors of calretinin and mesothelin to improve the diagnostic performance to detect malignant mesothelioma: results from a population-based cohort study. BMJ Open. 2017;7(10):e017104.
49. Creaney J, Olsen NJ, Brims F, Dick IM, Musk AW, de Klerk NH, et al. Serum mesothelin for early detection of asbestos-induced cancer malignant mesothelioma. Cancer Epidemiol Biomarkers Prev. 2010;19(9):2238–46.
50. Extended screening program for the early detection of occupational mesothelioma (EVA-Mesothel). https://www.dguv.de/ipa/eva-mesothel/index-2.jsp. (Accessed 21 October 2025).
51. Ray S, Patel SK, Kumar V, Damahe J, Srivastava S. Differential expression of serum/plasma proteins in various infectious diseases: specific or nonspecific signatures. Proteom Clin Appl. 2014;8(1–2):53–72.

Authors and Affiliations

Elton Jalis Herman[1] · Alessandra Allione[1] · Clara Viberti[1] · Marcello Manfredi[2] · Alessia Russo[1] · Khadija Sana-Hafeez[1] · Nina Kaiser[3] · Georg Johnen[3] · Thomas Brüning[3] · Dario Mirabelli[5] · Irma Dianzani[4,6] · Antonio Agudo[7,8] · Elisabete Weiderpass[9] · Vittorio Simeon[10] · Rudolf Kaaks[11] · Renée Turzanski-Fortner[11] · Rosario Tumino[12] · Lorenzo Milani[13] · José María Gálvez-Navas[14,15,16] · Matthias B. Schulze[17,18] · Catarina Schiborn[17,18,25] · Natalia Cabrera Castro[19,20] · Giovanna Masala[21] · Marcela Guevara[22,23,24] · Paolo Vineis[26] · Elisabetta Casalone[1] · Giuseppe Matullo[1,5,27]

✉ Elisabetta Casalone
elisabetta.casalone@unito.it

✉ Giuseppe Matullo
giuseppe.matullo@unito.it

[1] Department of Medical Sciences, University of Turin, Turin 10126, Via Santena 19, Italy

[2] Department of Translational Medicine, University of Piemonte Orientale, Novara 28100, Italy

[3] Institute for Prevention and Occupational Medicine of the German Social Accident Insurance (IPA), Institute of the Ruhr University Bochum, Bochum 44789, Germany

[4] Interdepartmental Center for Studies on Asbestos and Other Toxic Particulates "G. Scansetti", University of Turin, Turin 10126, Italy

[5] Unit of Cancer Epidemiology, Città della Salute e della Scienza University-Hospital and Center for Cancer Prevention (CPO), Turin 10126, Italy

[6] Department of Health Sciences, University of Eastern Piedmont, Novara 28100, Italy

[7] Unit of Nutrition and Cancer, Catalan Institute of Oncology-ICO, L' Hospitalet de Llobregat 08908, Spain

[8] Nutrition and Cancer Group,Epidemiology, Public Health, Cancer Prevention and Palliative Care Program, Bellvitge Biomedical Research [1]Institute-IDIBELL, L' Hospitalet de Llobregat 08908, Spain

[9] International Agency for Research on Cancer, World Health Organization, Lyon 69372, France

[10] Medical Statistics Unit, University of Naples "L. Vanvitelli", Naples 80138, Italy

[11] Division of Cancer Epidemiology, German Cancer Research Center (DKFZ), 69120 Heidelberg, Germany

[12] Hyblean Association for Epidemiology Research AIRE ONLUS, Ragusa 97100, Italy

[13] Centre for Biostatistics, Epidemiology, and Public Health, Department of Clinical and Biological Sciences, University of Turin, Turin 10043, Orbassano, Italy

[14] Escuela Andaluza de Salud Pública (EASP), Granada 18011, Spain

[15] Instituto de Investigación Biosanitaria ibs.GRANADA, Granada 18012, Spain

[16] Centro de Investigación Biomédica en Red de Epidemiología y Salud Pública (CIBERESP, Madrid 28029, Spain

[17] Department of Molecular Epidemiology, German Institute of Human Nutrition Potsdam-Rehbruecke, Nuthetal, Germany

[18] Institute of Nutritional Science, University of Potsdam, Nuthetal, Germany

[19] Department of Epidemiology, Regional Health Council, IMIB-Arrixaca, Murcia, Spain

[20] Spanish Consortium for Research on Epidemiology and Public Health (CIBERESP), Instituto de Salud Carlos III, Madrid, Spain

[21] Clinical Epidemiology Unit, Institute for cancer research, prevention and clinical network (ISPRO), Florence, Italy

[22] Instituto de Salud Pública y Laboral de Navarra, Pamplona 31003, Spain

[23] Centro de Investigación Biomédica en Red de Epidemiología y Salud Pública (CIBERESP, Madrid 28029, Spain

[24] Navarra Institute for Health Research (IdiSNA), Pamplona,)31008, Spain

[25] German Center for Diabetes Research, Neuherberg, Germany

[26] MRC Centre for Environment and Health, Imperial College London, St Mary's Campus, London, UK

[27] Medical Genetics Unit, AOU Città della Salute e della Scienza, urin 10126 T, Italy